

Supporting Information

Application of the YebF secretion pathway in *Escherichia coli* for rapid, on-plate screening of PETase libraries for improved activity

Jaeick Lee^{1*}, Maame Yaa Yamoah¹, Celina L. Bradley¹, Graeme Howe^{1*}, and David L. Zechel^{1*}

¹ Department of Chemistry, Queen's University, Kingston, ON, Canada

Supporting Information

Table of Contents

TABLES	4
Table S1. Primers used to amplify YebF-LCC specifying sequences with site-saturating mutations.....	4
Table S2. Primers used to amplify LCC specifying sequences lacking the YebF tag.....	4
FIGURES.....	5
Figure S1. Secretion of YebF-LCC from <i>Escherichia coli</i> BL21 (DE3) indicated by a BHET zone clearing assay	5
Figure S2. Identification of active-site proximal residues in LCC using HotSpot Wizard	6
Figure S3. Comparison of glide gscore's LCC mutant docking structures with PET dimer and trimer.....	7
Figure S4. Screening for more active YebF-LCC-V212X variants using a BHET zone of clearance assay.....	8
Figure S5. Screening for more active YebF-LCC-Y95X and L102X variants using a BHET zone clearing assay	9
Figure S6. Multiple sequence alignment of YebF-LCC-Y95F from colony #42.....	10
Figure S7. Screening for more active YebF-LCC-V212T-L102X variants using a BHET zone of clearance assay.....	12
Figure S8. Comparison of clearance zone formation by <i>E. coli</i> colonies expressing YebF-LCC and LCC variants on BHET supplemented agar plates	13
Figure S9. Verification of the expression for YebF-LCC variants in <i>E. coli</i> in LB autoinduction media.....	14
Figure S10. Determination of T _m values for LCC WT, V212T, and L102F-V212T by UV absorbance	15
Figure S11. Michaelis-Menten plot of LCC variants using pNPB as substrate	16
Figure S12. Hill plot analysis of LCC variants using 3PET	17
Figure S13. Docking models of 3PET with LCC variants	18
Figure S14. Glide gscores of 3PET-LCC mutant docking models.....	19
Figure S15. Comparison of protein surface hydrophobicity and polarity in 3PET-LCC mutant docking models.....	20
Figure S16. Protein surface analysis of docking models of 3PET with LCC variants.....	21
Figure S17. Plasmid map of pD421- <i>YebF</i> -WT-LCC	22
Figure S18. Plasmid sequence for pD421- <i>YebF</i> -WT-LCC	23

Supporting Information

Figure S19. Structural alignment of LCC crystal and AlphaFold3-predicted models25

Supporting Information

TABLES

Table S1. Primers used to amplify YebF-LCC specifying sequences with site-saturating mutations

Primer	Sequence (5' → 3')
Y95X-Fwd	GCAATGTCTCCGGGTNNNACGGCAGATGCGAGC
Y95X-Rev	GCTCGCATCTGCCGTNNNACCCGGAGACATTGC
L102X-Fwd	GATGCGAGCTCTNNNGCGTGGCTGGGTC
L102X-Rev	GACCCAGCCACGCNNNAGAGCTCGCATC
V212X-Fwd	GAAGCGGATACGNNNGCACCAGTCAGCC
V212X-Rev	GGCTGACTGGTGCNNNCGTATCCGCTTC

Table S2. Primers used to amplify LCC specifying sequences lacking the YebF tag

Primer	Sequence (5' → 3') ^a
LCC-Nc-F	ATTCAGTCCCAT TGGG CAATCCGTACC
LCC-Xh-R	ATTCAGT CCTCGAG CTGGCAGTGACGG

^aRestriction enzyme recognition sites shown in bold.

Supporting Information

FIGURES

Figure S1. Secretion of YebF-LCC from *Escherichia coli* BL21 (DE3) indicated by a BHET zone clearing assay

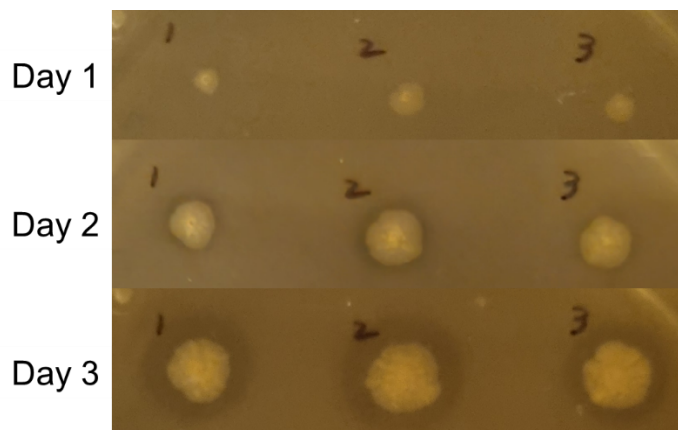


Figure S1. Secretion of YebF-LCC from *Escherichia coli* BL21 (DE3) indicated by a BHET zone clearing assay. *E. coli* colonies expressing the gene specifying YebF-LCC were grown on LB auto-induction agar plates supplemented with 5 mM BHET. The plate was incubated at 37°C for three days following inoculation with three single colonies.

Supporting Information

Figure S2. Identification of active-site proximal residues in LCC using HotSpot Wizard

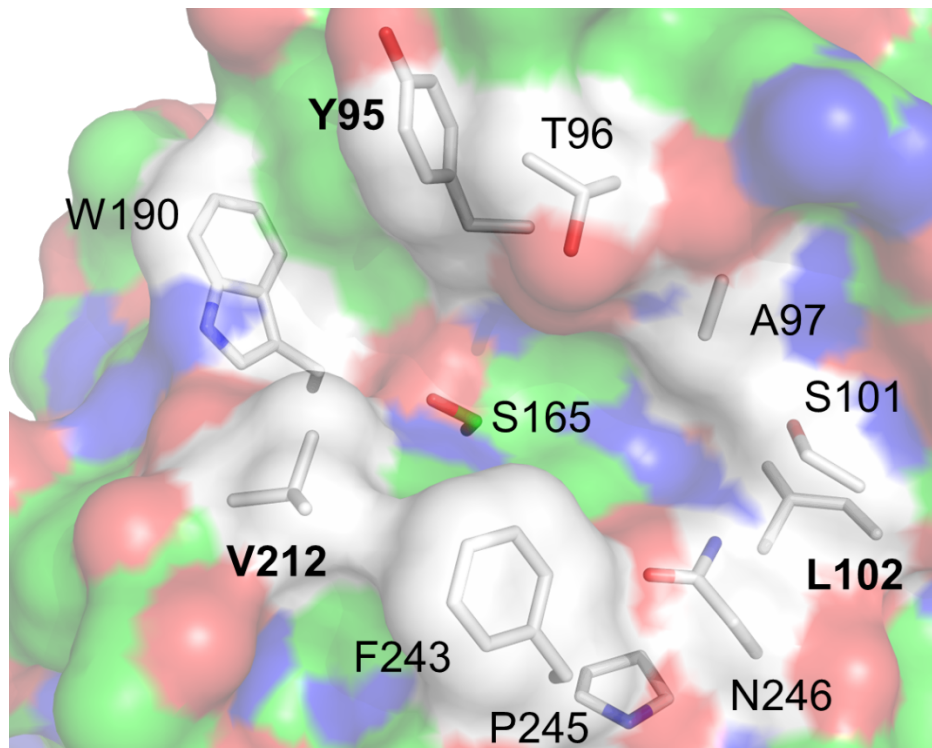


Figure S2. Identification of active-site proximal residues in LCC using HotSpot Wizard. Residues located in or near the active site of wild-type (WT) LCC, as predicted by HotSpot Wizard, are shown in white. The catalytic residue S165 is highlighted in green. Residues selected for site-saturation mutagenesis are indicated in bold. The analysis was performed using the AlphaFold3-predicted structure of WT LCC as the input template.

Supporting Information

Figure S3. Comparison of glide gscores LCC mutant docking structures with PET dimer and trimer

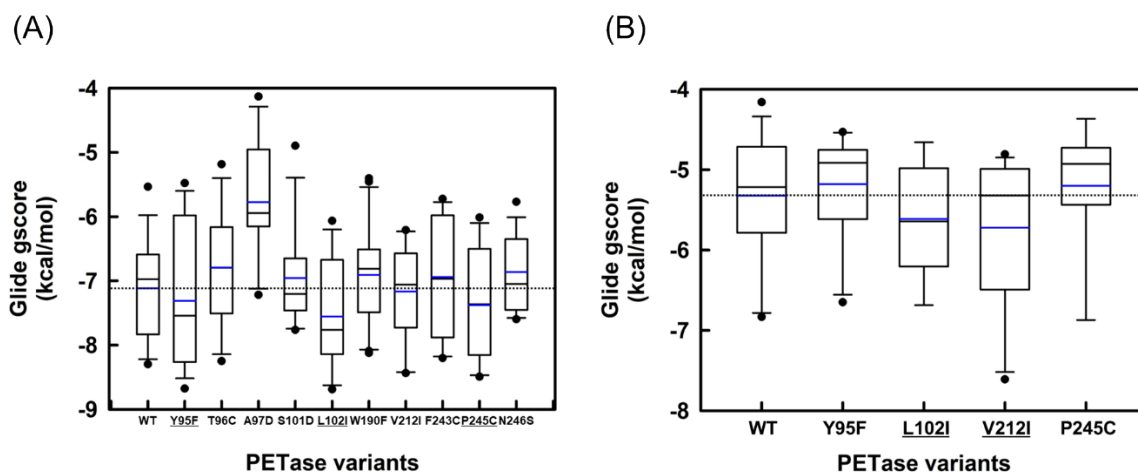


Figure S3. Comparison of Glide gscores for LCC mutant docking with PET dimer and trimer. Docking scores of LCC mutants, as suggested by HotSpot Wizard (Fig. S2), are shown for PET trimer (A) and PET dimer (B). The average and median Glide gscores of wild-type (WT) and mutant enzymes are indicated by blue and black lines, respectively. Mutants exhibiting higher average scores than WT are underlined. All mutant structures were generated using AlphaFold3.

Supporting Information

Figure S4. Screening for more active YebF-LCC-V212X variants using a BHET zone of clearance assay

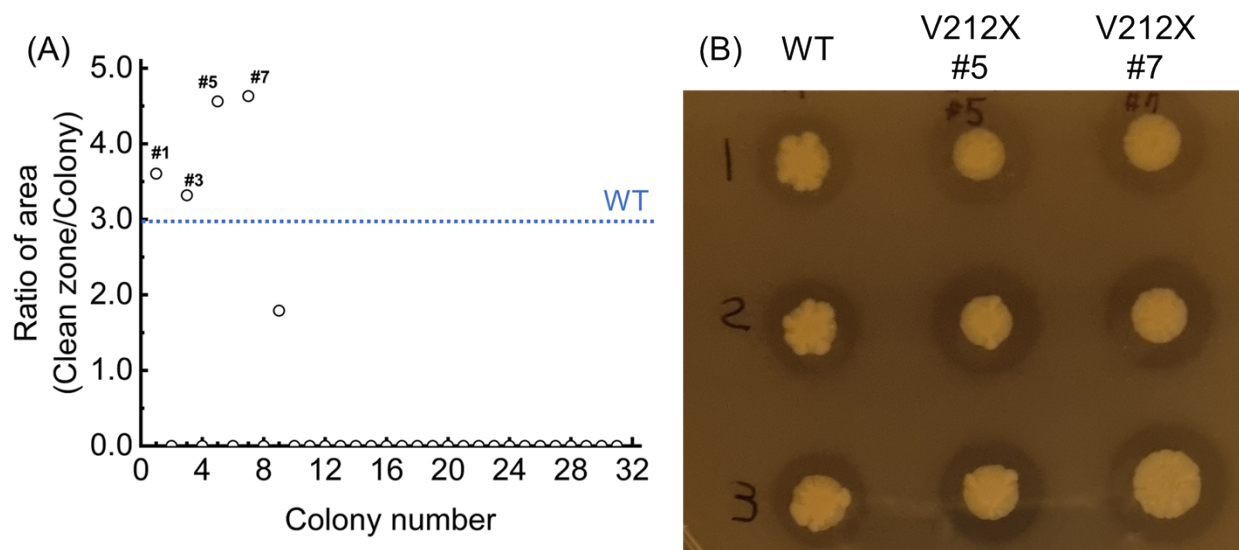


Figure S4. Screening for more active YebF-LCC-V212X variants using a BHET zone of clearance assay. (A) Random *E. coli* colonies (31 total) expressing YebF-LCC variants V212X supplemented with 0.025% glycine and 5 mM BHET. The clearance ratio value for wild-type (WT) YebF-LCC is represented by a blue dashed line. (B) Selected colonies from A were used to grow an overnight culture in LB liquid media. An aliquot of each culture (1 μ L) was spotted on an LB auto-induction agar plate supplemented with 0.025% glycine and 5 mM BHET. The plate was incubated at 30°C for one day, followed by 42°C for one day.

Supporting Information

Figure S5. Screening for more active YebF-LCC-Y95X and L102X variants using a BHET zone clearing assay

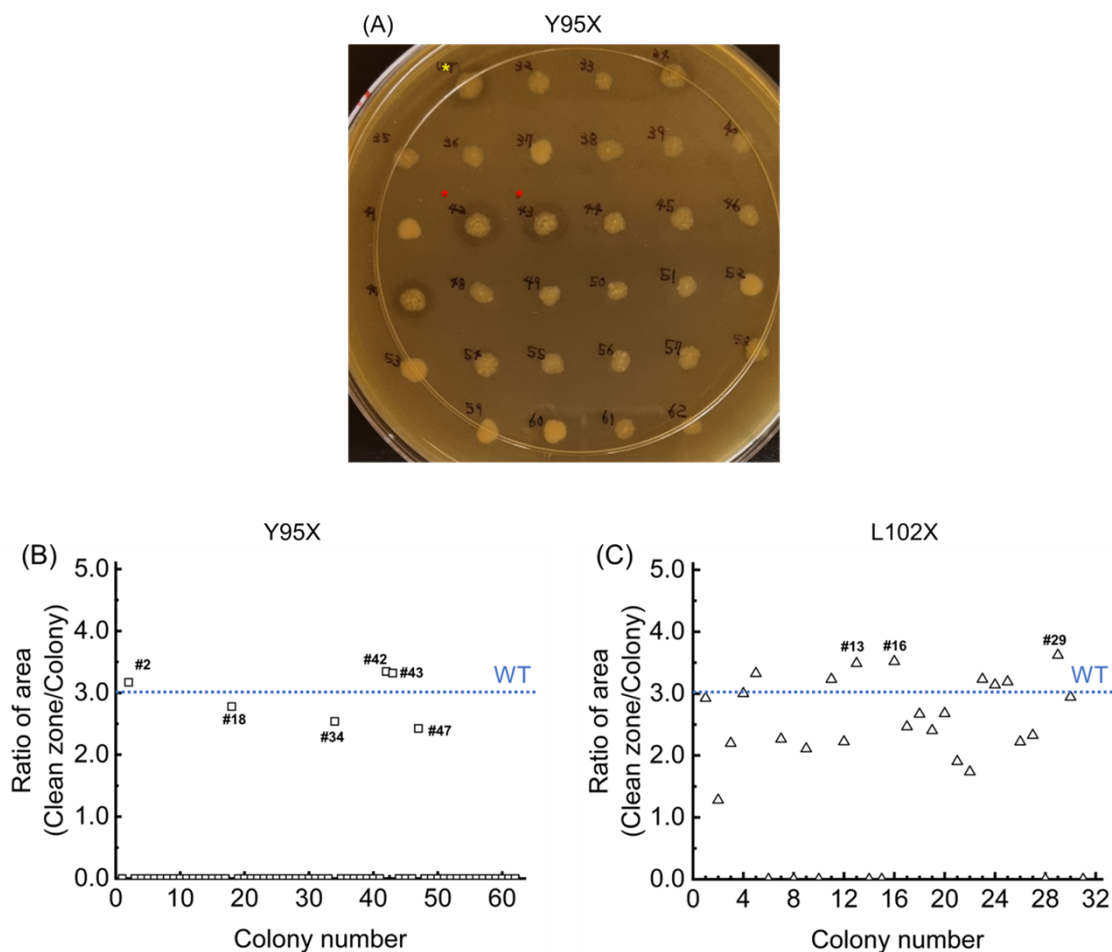


Figure S5. Screening for more active YebF-LCC Y95X and L102X variants using a BHET zone clearing assay. Shown are more colonies expressing YebF-LCC single-site variants derived from site-saturated mutagenesis of residues Y95 (A). *E. coli* colonies expressing the variants were incubated on LB auto-induction agar plates supplemented with 0.025% glycine and 5 mM BHET. The plates were incubated at 30°C for one day, followed by 42°C for one day. Colonies expressing variants more active than wild-type (WT) YebF-LCC (yellow asterisk) are marked with a red asterisk. Random *E. coli* colonies (62 and 31 total) expressing YebF-LCC variants Y95X (B) and L102X (C) were grown on LB auto-induction agar plates supplemented with 0.025% glycine and 5 mM BHET. The ratio for WT YebF-LCC is represented by a blue dashed line.

Supporting Information

Figure S6. Multiple sequence alignment of YebF-LCC-Y95F from colony #42

```
WT          ATGAAAAGCGTGGTGCATTCTGGGTCTGCTCCTGGTCAGCGCCTGTGCATCGGTGTTT
Y95X#42    ATGAAAAGCGTGGTGCATTCTGGGTCTGCTCCTGGTCAGCGCCTGTGCATCGGTGTTT
*****

WT          GCGGCGAACAATGAAACCAGCAAGAGCGTCACCTTCCCTAAATGCGAAGATCTGGATGCT
Y95X#42    GCGGCGAACAATGAAACCAGCAAGAGCGTCACCTTCCCTAAATGCGAAGATCTGGATGCT
*****

WT          GCGGGTATTGCGGCTAGCGTTAAGCGTGACTACCAGCAGAACC GTTGGCGCTGGGCG
Y95X#42    GCGGGTATTGCGGCTAGCGTTAAGCGTGACTACCAGCAGAACC GTTGGCGCTGGGCG
*****

WT          GACGACCAGAAAATTGTGGGTCAAGCCGATCCAGTCGCATGGGTGAGCCTGCAAGACATT
Y95X#42    GACGACCAGAAAATTGTGGGTCAAGCCGATCCAGTCGCATGGGTGAGCCTGCAAGACATT
*****

WT          CAGGGTAAAGACGACAAGTGGAGCGTTCGCTGACTGTTCTGGCAAGAGCGCTGATATC
Y95X#42    CAGGGTAAAGACGACAAGTGGAGCGTTCGCTGACTGTTCTGGCAAGAGCGCTGATATC
*****

WT          CATTACCAAGTCAGCGTCGACTGCAAGGCCGGTATGGCCGAGTACCAACGCCGTCACATG
Y95X#42    CATTACCAAGTCAGCGTCGACTGCAAGGCCGGTATGGCCGAGTACCAACGCCGTCACATG
*****

WT          AGCAATCCGTACCAGCGTGGTCCGAATCCGACCCGACGCGCTGACCGCGGACGGCCCG
Y95X#42    AGCAATCCGTACCAGCGTGGTCCGAATCCGACCCGACGCGCTGACCGCGGACGGCCCG
*****

WT          TTCAGCGTGGCAACCTATACCGTGAGCCGCTTGAGCGTGAGCGGTTTCGGTGGCGCGTT
Y95X#42    TTCAGCGTGGCAACCTATACCGTGAGCCGCTTGAGCGTGAGCGGTTTCGGTGGCGCGTT
*****

WT          ATCTATTACCCGACGGGCACGAGCCTGACCTTCGGTGGCATTGCAATGTCTCCGGTTAC
Y95X#42    ATCTATTACCCGACGGGCACGAGCCTGACCTTCGGTGGCATTGCAATGTCTCCGGTTTTT
*****

WT          ACGGCAGATGCGAGCTCTTTAGCGTGGCTGGGTCGCGGCCTGGCCTGCGACGGCTTTGTA
Y95X#42    ACGGCAGATGCGAGCTCTTTAGCGTGGCTGGGTCGCGGCCTGGCCTGCGACGGCTTTGTA
*****

WT          GTTTTGGTGATCAACACTAATAGCGTTTTGACTATCCGACTCACGTGCGTCCCAGCTG
Y95X#42    GTTTTGGTGATCAACACTAATAGCGTTTTGACTATCCGACTCACGTGCGTCCCAGCTG
*****

WT          AGCGCGGCACTGAACTATCTGCGTACGTCCAGCCCAGCGCGTTTCGTGCGCGCTTGAT
Y95X#42    AGCGCGGCACTGAACTATCTGCGTACGTCCAGCCCAGCGCGTTTCGTGCGCGCTTGAT
```

Supporting Information

```

*****
WT          GCGAATCGTCTGGCCGTCGCGGGTCACAGCATGGGTGGCGGGCAGCAGCTGAGAATCGCG
Y95X#42    GCGAATCGTCTGGCCGTCGCGGGTCACAGCATGGGTGGCGGGCAGCAGCTGAGAATCGCG
*****

WT          GAGCAAACCCGTCCCTTAAAGCTGCGGTGCCGCTGACCCCTTGGCAGACCGATAAAACC
Y95X#42    GAGCAAACCCGTCCCTTAAAGCTGCGGTGCCGCTGACCCCTTGGCAGACCGATAAAACC
*****

WT          TTCAATACCTCTGTGCCGTTCTGATTGTCGGTGCTGAAGCGGATACGGTCGCACCAGTC
Y95X#42    TTCAATACCTCTGTGCCGTTCTGATTGTCGGTGCTGAAGCGGATACGGTCGCACCAGTC
*****

WT          AGCCAGCATGCAATTCGGTTTTATCAAATCTGCCGTCCACGACCCCGAAAGGTACGTT
Y95X#42    AGCCAGCATGCAATTCGGTTTTATCAAATCTGCCGTCCACGACCCCGAAAGGTACGTT
*****

WT          GAGCTGGATAATGCGAGCCACTTTGCACCGAATCCAATAACGCAGCCATCAGCGTGAC
Y95X#42    GAGCTGGATAATGCGAGCCACTTTGCACCGAATCCAATAACGCAGCCATCAGCGTGAC
*****

WT          ACCATCTCTTGGATGAAGCTGTGGGTTGATAACGACACCCGCTATCGTCAATTCTTGTGT
Y95X#42    ACCATCTCTTGGATGAAGCTGTGGGTTGATAACGACACCCGCTATCGTCAATTCTTGTGT
*****

WT          AACGTTAACGATCCGGCGCTGAGCGACTTTCGTACGAACAACCGTCACTGCCAGCATCAC
Y95X#42    AACGTTAACGATCCGGCGCTGAGCGACTTTCGTACGAACAACCGTCACTGCCAGCATCAC
*****

WT          CATCATCACCCTGA
Y95X#42    CATCATCACCCTGA
*****

```

Figure S6. Multiple sequence alignment of YebF-LCC-Y95F from colony #42. The mutation Y95F (TAC→TTT) is highlighted in yellow. Asterisks denote fully conserved residues. The plasmid sequences of the wild type and the double mutant were aligned using CLUSTALW.

Supporting Information

Figure S7. Screening for more active YebF-LCC-V212T-L102X variants using a BHET zone of clearance assay

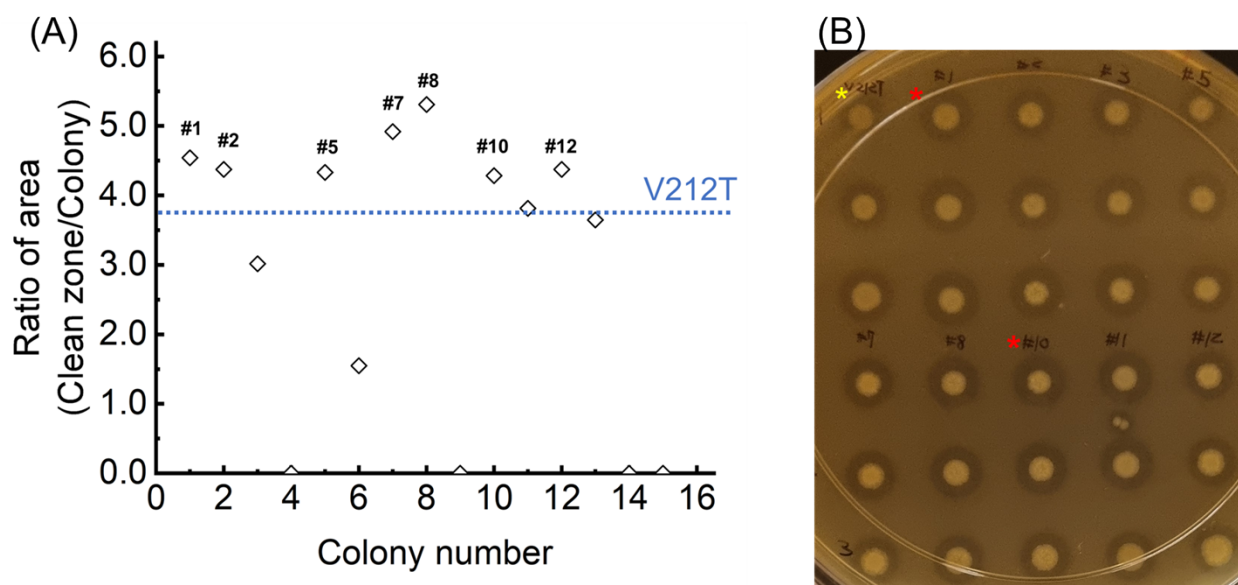


Figure S7. Screening for more active YebF-LCC-V212T-L102X variants using a BHET zone of clearance assay. (A) Random *E. coli* colonies (15 total) expressing YebF-LCC variants V212T-L102X supplemented with 0.025% glycine and 5 mM BHET. The clearance ratio value for YebF-LCC V212T is represented by a blue dashed line. (B) Selected colonies from A were used to grow an overnight culture in LB liquid media. An aliquot of each culture (1 μ L) was spotted on an LB auto-induction agar plate supplemented with 0.025% glycine and 5 mM BHET. The plate was incubated at 30°C for one day, followed by 42°C for one day. The mutants with the highest and second-highest ratios are greater than those of the YebF-LCC V212T control (yellow asterisk) is marked with a red asterisk.

Supporting Information

Figure S8. Comparison of clearance zone formation by *E. coli* colonies expressing YebF-LCC and LCC variants on BHET supplemented agar plates

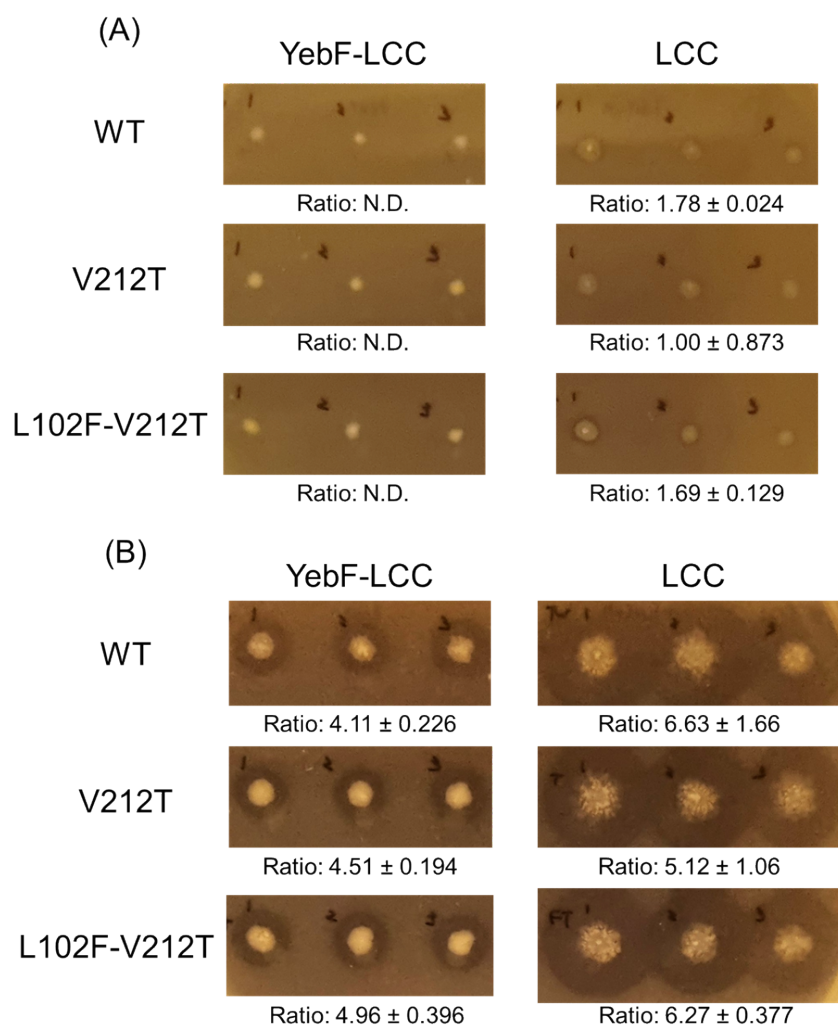


Figure S8. Comparison of clearance zone formation by *E. coli* colonies expressing YebF-LCC and LCC variants on BHET supplemented agar plates. *E. coli* colonies expressing YebF-LCC and LCC variants were incubated on LB auto-induction agar plates supplemented with 0.025% glycine and 5 mM BHET. The plates were incubated at 30°C for one day (A), followed by 42°C for one day (B). The areas of the clearance zones and the corresponding colonies were measured with ImageJ and expressed as ratios. The promiscuous cell-hydrolyzing activity of LCC results in less defined colonies, and correspondingly, more significant uncertainties in the ratios of clearance halo size to colony size.

Supporting Information

Figure S9. Verification of the expression for YebF-LCC variants in *E. coli* in LB autoinduction media

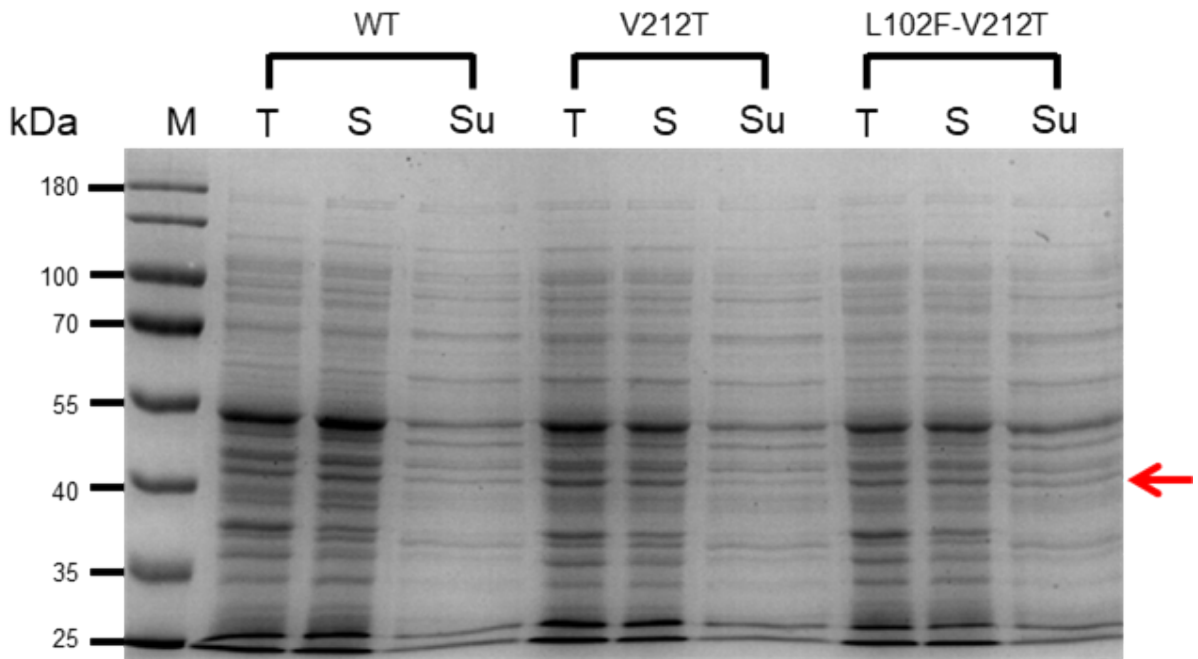


Figure S9. Expression of YebF-LCC variants in *E. coli* in LB autoinduction media. *E. coli* BL21 (DE3) harbouring pD421-*YebF-LCC* variants was cultured in LB autoinduction medium supplemented with 0.025% glycine at 30 °C with shaking at 180 rpm for 48 h. The predicted YebF-LCC (41.8 kDa) is indicated by the red arrow. Lane T: total cellular protein; lane S: soluble cellular protein; lane Su: culture supernatant.

Figure S10. Determination of T_m values for LCC WT, V212T, and L102F-V212T by UV absorbance

Supporting Information

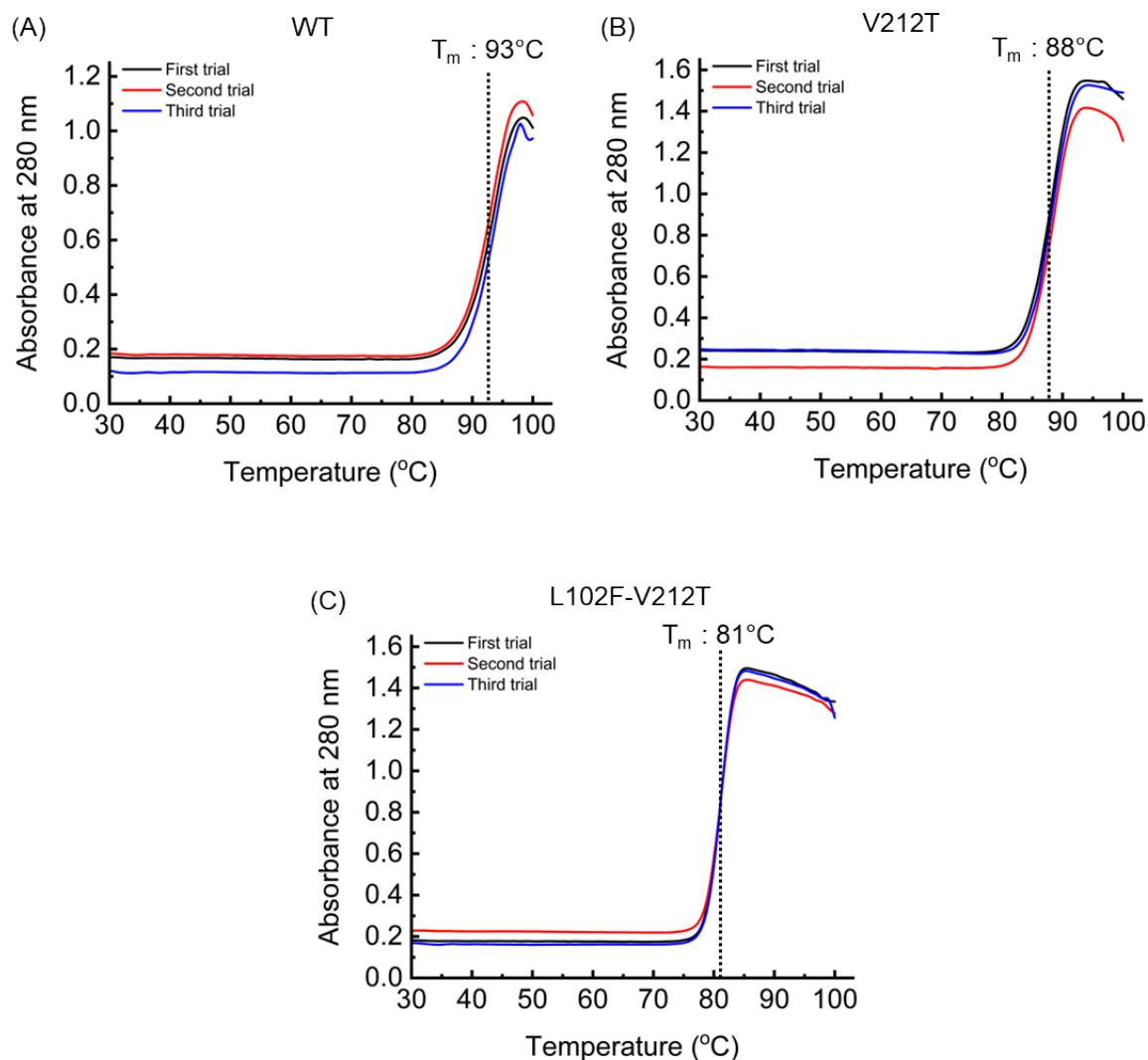


Figure S10. Determination of T_m values for LCC WT, V212T, and L102F-V212T by UV absorbance. Samples (0.2 mg/mL) of (A) LCC WT, (B) V212T, and (C) L102F-V212T were monitored at 280 nm across a temperature range of 25 to 105 °C, with a heating rate of 10 °C/min. The melting temperature (T_m) was determined as the midpoint of the highest absorbance value, indicated by a vertical black dashed line.

Supporting Information

Figure S11. Michaelis-Menten plot of LCC variants using *p*NPB as substrate

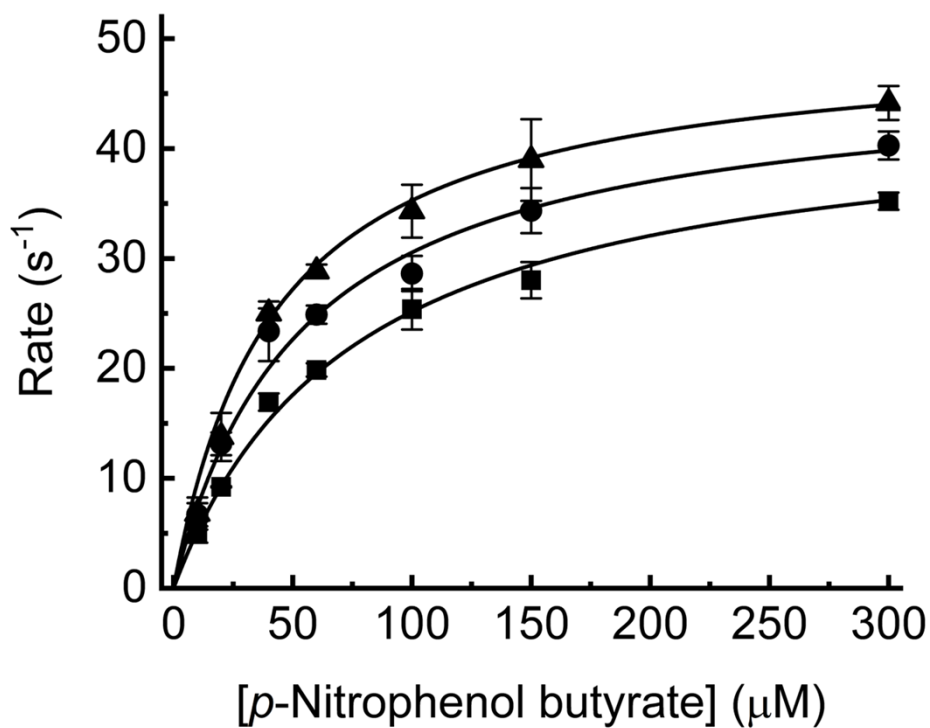


Figure S11. Michaelis-Menten plot of LCC variants using *p*NPB as substrate. Michaelis-Menten plots for WT (circles), V212T (triangles), and L102F-V212T (squares) were generated under identical buffer conditions at 45 °C. Data points represent the mean of triplicate measurements. Kinetic parameters (k_{cat} and K_{M}) were derived by fitting the data to the Michaelis-Menten equation (Table 1).

Supporting Information

Figure S12. Hill plot analysis of LCC variants using 3PET

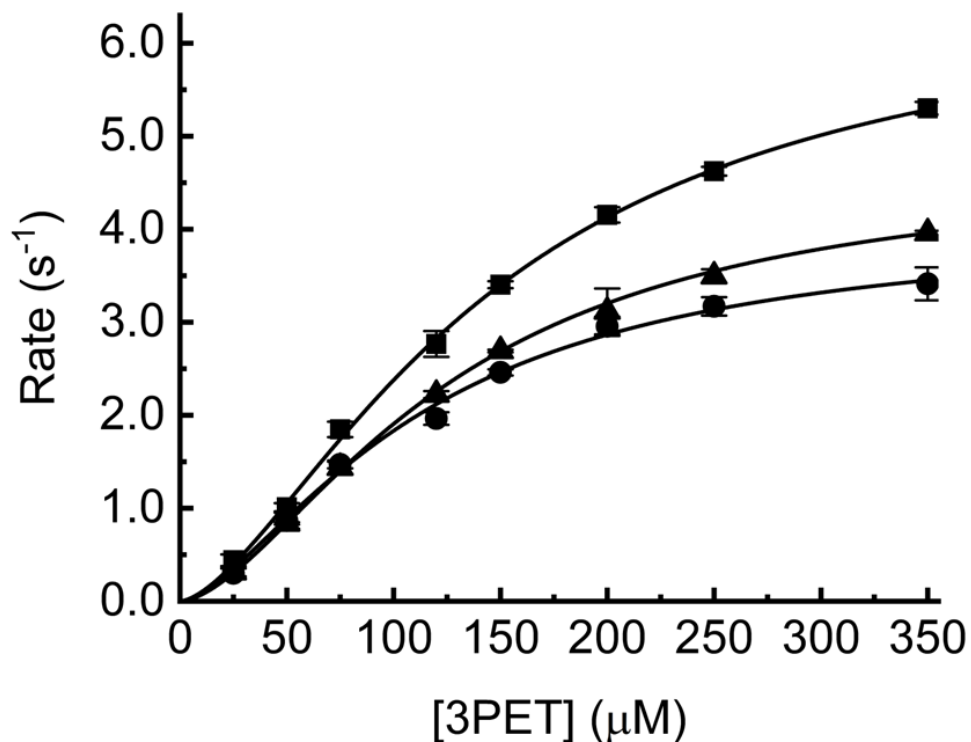


Figure S12. Hill plot analysis of LCC variants using 3PET. Hill plots for WT (circles), V212T (triangles), and L102F-V212T (squares) were generated using variable concentrations of 3PET under identical buffer and temperature conditions. Turbidity was measured at 600 nm. All data points represent the mean of triplicate measurements. Kinetic parameters (k_{cat} , K_M , and Hill coefficient n) were obtained by fitting the data to the Hill equation (Table 2).

Figure S13. Docking models of 3PET with LCC variants

Supporting Information

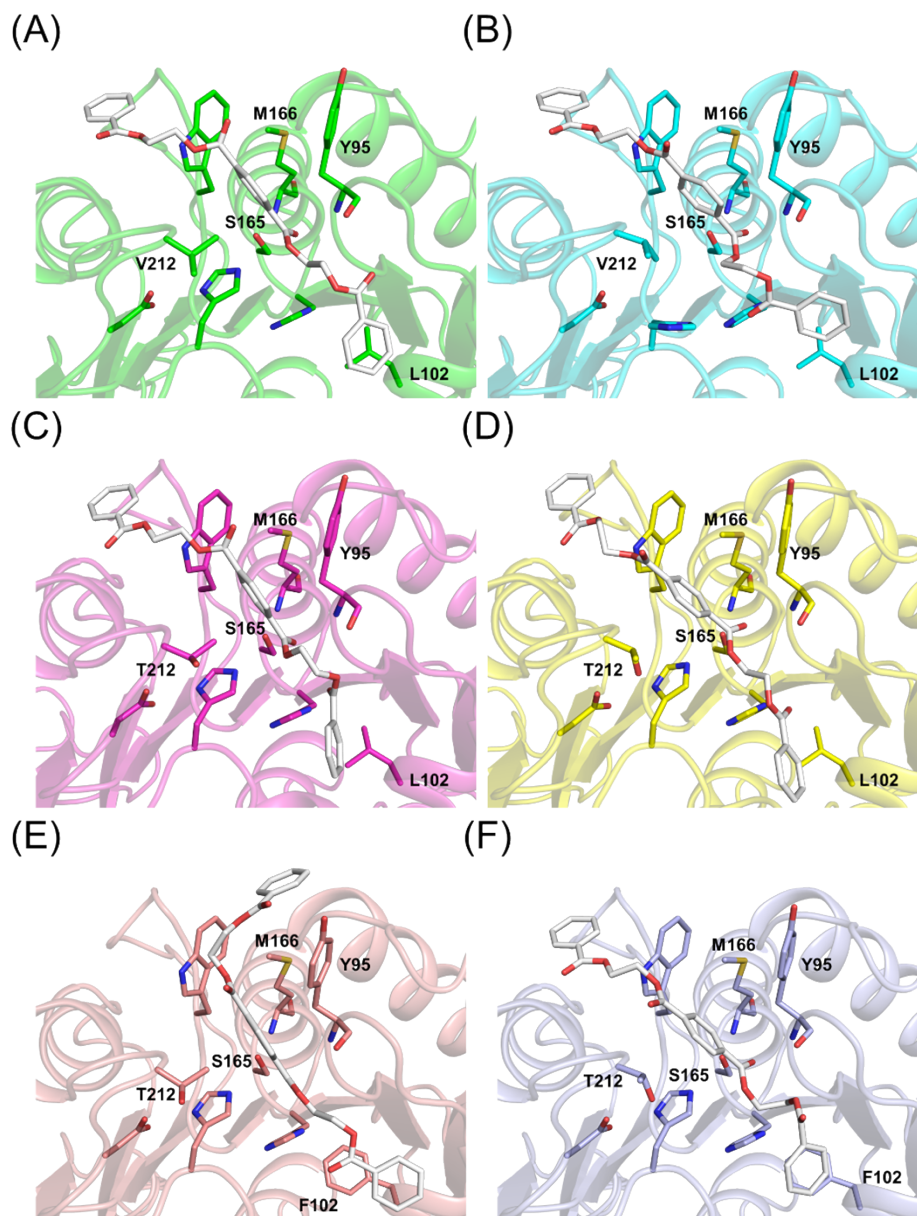


Figure S13. Docking models of 3PET with LCC variants. Docking poses of 3PET with wild-type and mutant LCC enzymes are shown. Wild-type LCC with Val212 in horizontal and vertical conformations (A, B), respectively. V212T mutant with Thr212 in horizontal and vertical conformations (C, D). L102F-V212T double mutant with Thr212 in horizontal and vertical conformations (E, F). 3PET molecules are shown in white. Catalytic pocket residues are labelled in bold.

Figure S14. Glide gscores of 3PET-LCC mutant docking models

Supporting Information

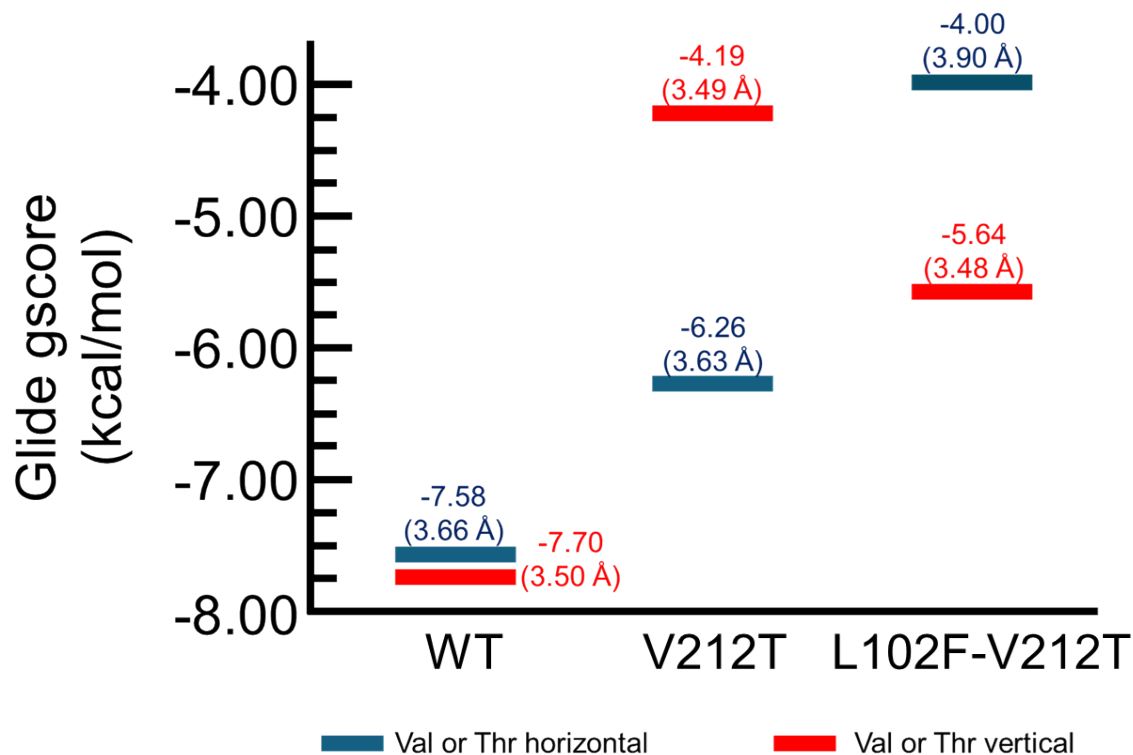


Figure. S14. Glide gscores for 3PET-LCC mutant docking models. Docking models of wild-type LCC (WT), V212T, and L102F-V212T were evaluated based on Glide gscores. Models featuring Val or Thr residues in a horizontal conformation are shown in blue, while those with vertical conformations are shown in red. For each model, the distance between the catalytic residue S165 and the carbonyl carbon of 3PET is indicated in brackets alongside the corresponding Glide gscore. Associated structural representations are provided in Fig. S13.

Supporting Information

Figure S15. Comparison of protein surface hydrophobicity and polarity in 3PET-LCC mutant docking models

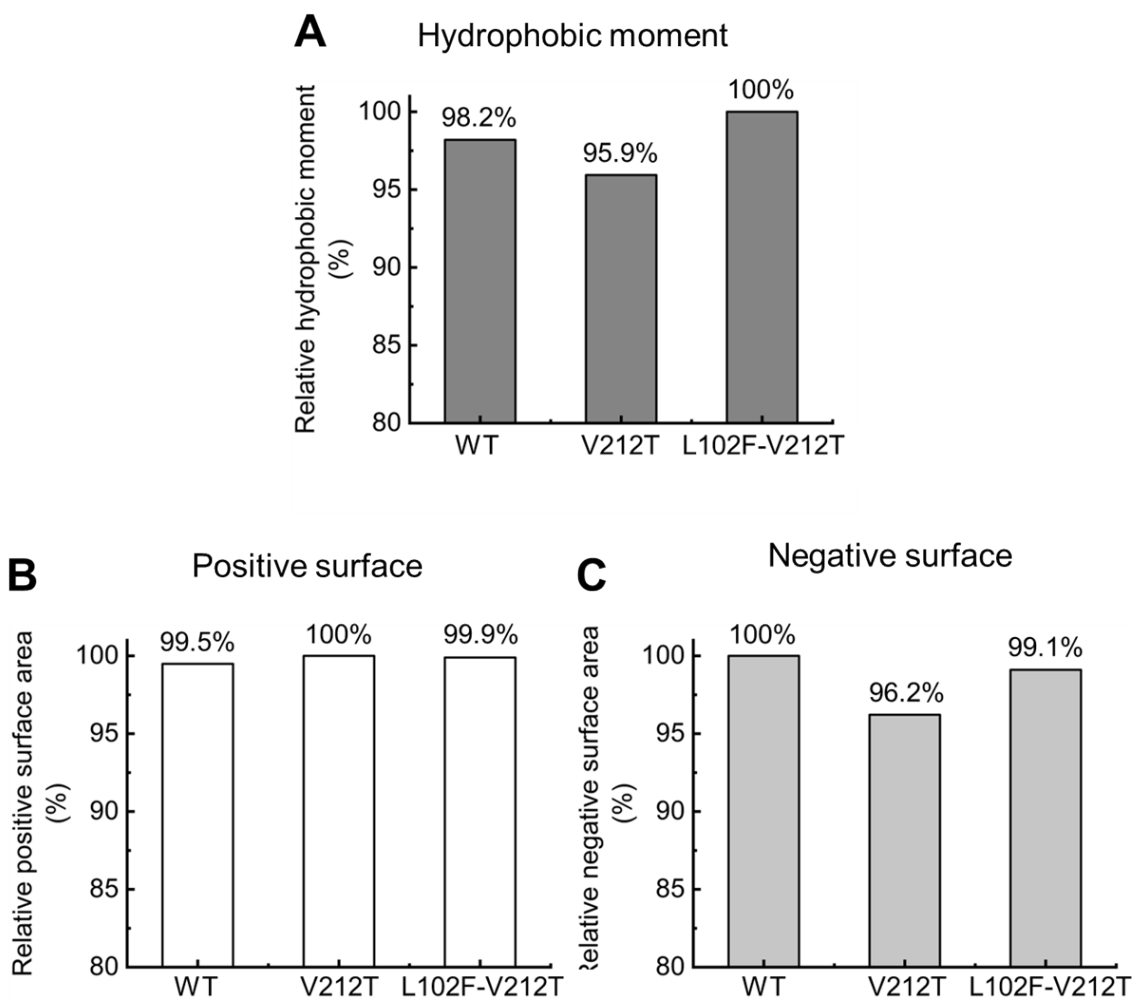


Figure S15. Comparison of protein surface hydrophobicity and polarity in 3PET-LCC mutant docking models. Surface properties of three docking models were analyzed: 3PET-wild-type LCC with horizontal V212 conformation (WT), 3PET-V212T mutant with vertical T212 conformation (T), and 3PET-L102F-V212T double mutant with vertical T212 conformation (FT). (A) Hydrophobicity, (B) positive surface charge, and (C) negative surface charge were evaluated across the entire enzyme surface. Hydrophobic moments and surface charge distributions were calculated using the Protein Surface Analyzer module in Schrödinger Maestro. Corresponding structural overlays with surface hydrophobicity and polarity mapping are presented in Fig. S16.

Supporting Information

Figure S16. Protein surface analysis of docking models of 3PET with LCC variants

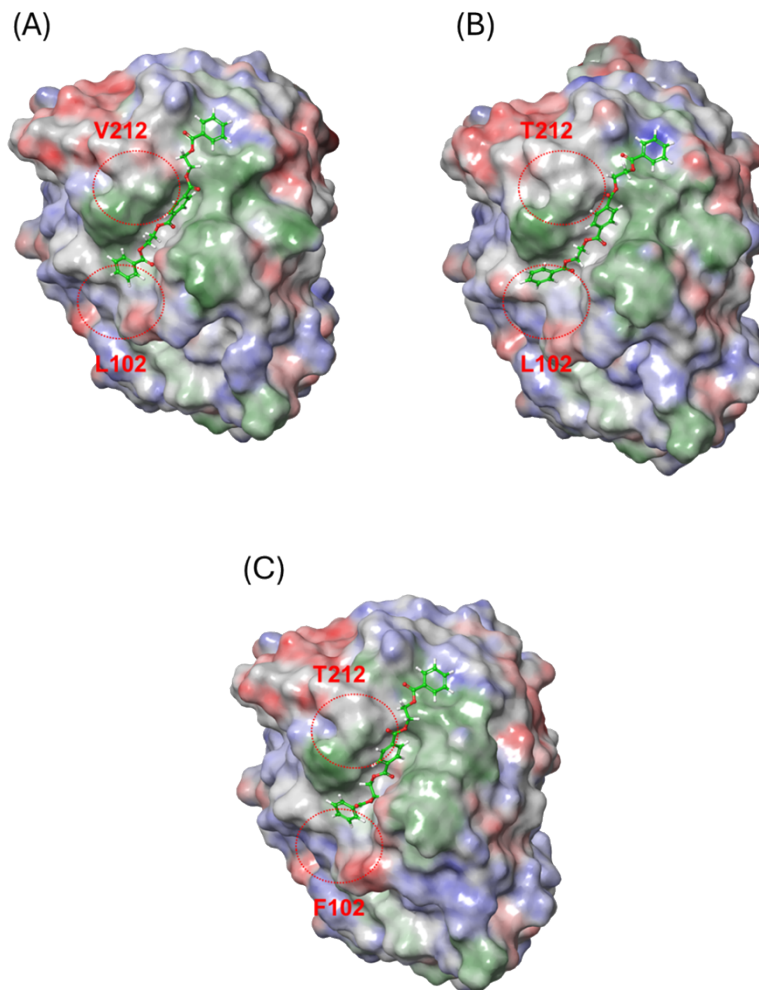


Figure S16. Protein surface analysis of 3PET–LCC docking models. Surface properties were analyzed for three docking models including 3PET-wild type-LCC with horizontal V212 conformation (A), 3PET-V212T mutant with vertical T212 conformation (B), and 3PET-L102F-V212T double mutant with vertical T212 conformation (C). The 3PET molecules are shown in green, and surface patches are color coded with blue indicating positive charge, red indicating negative charge, and dark green representing hydrophobic regions. Mutation sites including V or T212 and L or F102 are highlighted with red circles.

Supporting Information

Figure S17. Plasmid map of pD421-*YebF*-WT-LCC

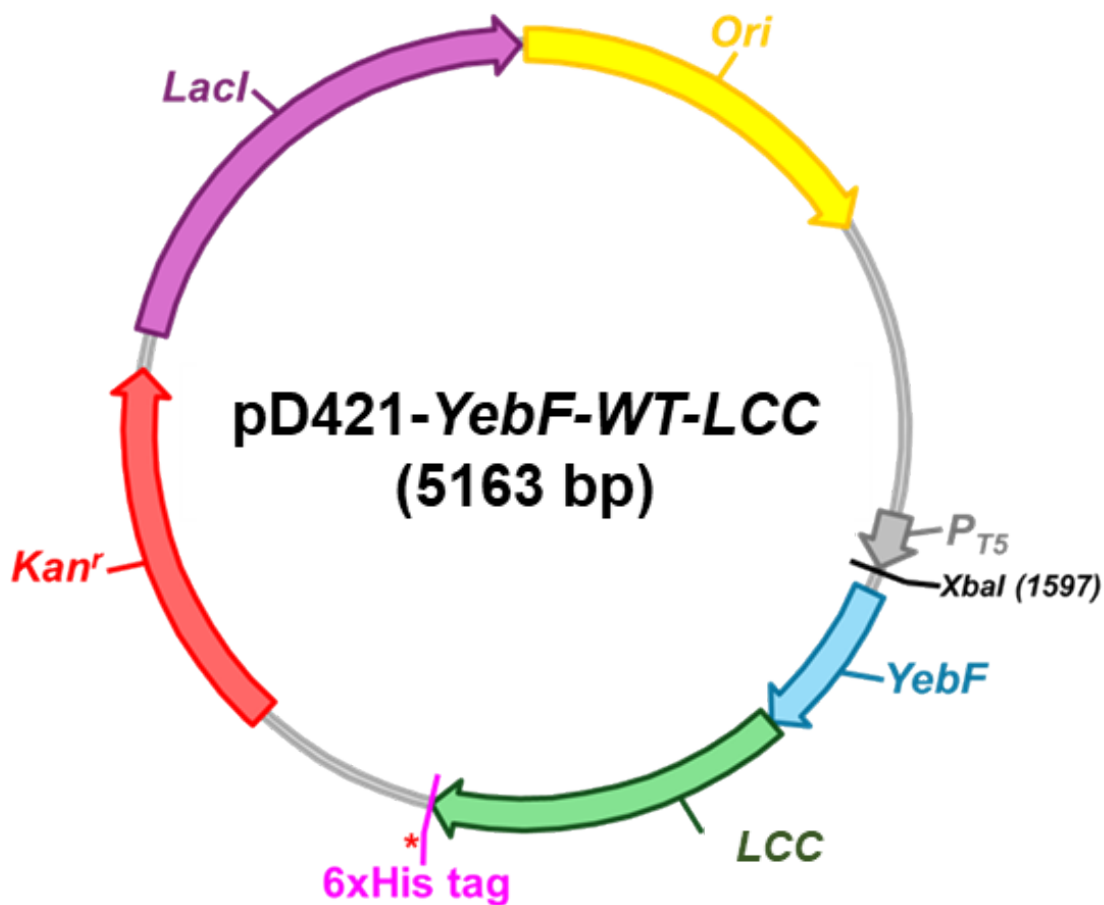


Figure S17. Plasmid map for pD421-*YebF*-WT-LCC. *YebF* and *LCC* genes are indicated. The DNA sequence from the T5 promoter to the termination codon are shown. Abbreviations: *Kan^r* (kanamycin resistance), *LacI* (lac repressor), *Ori* (origin), *P_{T5}* (T5 promoter), *6xHis tag* (six histidine tag). The sequence is shown in Figure S18.

Supporting Information

Figure S18. Plasmid sequence for pD421-*YebF*-WT-LCC

TTAATAAGATGATCTTCTTGAGATCGTTTTGGTCTGCGCGTAATCTCTTGCTCTGAAAACGAAAAAACC GCCTTGCA
GGGCGGTTTTTCGAAGTTCTCTGAGCTACCAACTCTTTGAACCGAGGTAACCTGGCTTGGAGGAGCGCAGTCACCA
AAACTTGTCTTTTACAGTTTAGCCTTAACCGGCGCATGACTTCAAGACTAACCCTCTAAATCAATTACAGTGGCTG
CTGCCAGTGGTGCTTTTGCATGTCTTTCCGGGTTGGACTCAAGACGATAGTTACCGGATAAGGCGCAGCGGTTCGGA
CTGAACGGGGGGTTCGTGCATACAGTCCAGCTTGGAGCGAACTGCCTACCCGGAAGTGAAGTGTGAGGCGTGGAAAT
GAGACAAACGCGGCCATAACAGCGGAATGACACCGGTAACCCGAAAGGCAGGAACAGGAGAGCGCACGAGGGA
GCCGCCAGGGGAAACGCCTGGTATCTTTATAGTCTGTGCGGTTTCGCCACCACTGATTTGAGCGTCAGATTTTCG
TGATGCTTGTGAGGGGGGCGGAGCCTATGGAAAAACGGCTTTGCCGCGGCCCTCTCACTTCCCTGTAAAGTATCTT
CCTGGCATCTTCCAGGAAATCTCCGCCCCGTTGTAAGCCATTTCCGCTCGCCGACGTCGAACGACCGAGCGTAGC
GAGTCAGTGAGCGAGGAAGCGGAATATATCTGTATCACATATTCTGCTGACGCACCGGTGCAGCCTTTTTTCTCC
TGCCACATGAAGCACTTCACTGACACCCTCATCAGTGCCAACATAGTAAGCCAGTATACACTCCGCTAGCGCTG

Origin (p15a)

AGGTCCCGCAGCCGACGACCGAGCGCAGTCAGTGAGCGAGGAAGCGGAAGGCGAGAGTAGGGAAGTGC
AGGCATCAAATAAGCAGAAGGCCCTGACGGATGGCCTTTTTGCGTTTCTACAAACTCTTTCTGTGTTGTA
GACGGCCAGTCTTAAGCTCGGGCCCCCTGGGCGGTTCTGATAACGAGTAATCGTTAATCCGCAATAACGTA
ACCCGCTTCGGCGGGTTTTTTTTATGGGGGAGTTTGGGAAAGAGCATTGTGTCAGAATATTTAAGGGCGCCTGTCA
CTTTGCTTGATATATGAGAATTATTTAACCTTATAAATGAGAAAAAGCAACGCACCTTTAATAAGATACGTTGCT
TTTTCGATTGATGAACACCTATAATTAACCTATTCATCTATTATTTATGATTTTTGTATATACAATATTTCTAGTTT
GTTAAAGAGAATTAAGAAAAATAATCTCGAAAAATAAAGGGAAAAATCAGTTTTTGTATACAAAATTATACATG
TCAACGATAATACAAAATAAATAACAACTATAAGATGTTATCAGTATTTATGATTTAGATAAAATTTTGTG
CGCCCTTACACGTAAGTGTGCTGAAAAATTGTGAGCGGATAACAATTACGAGCTTACATGCACAGTTAAATCAT
AAAAATTTATTTGCTTTGTGAGCGGATAACAATTATAATATGTGGAATTGTGAGCGCTCACAATTCACAACGGTT
TCCCTCTAGAATAATTTTGT

T5 promoter

XbaI

TTAACTTTTAGAGACCAAGGAGGTAAAAAATGAAAAAGCGTGGTGCATTCTGGGTCTGCTCCTGGTCAGCGCCTG
TGCATCGGTGTTTGCGGCGAACAAATGAAACCAGCAAGAGCGTCACCTTCCCTAAAATGCGAAGATCTGGATGCTGC
GGGTATTGCGGCTAGCGTTAAGCGTGACTACCAGCAGAACCGTGTGCGCGCTGGGCGGACGACCAGAAAAATGT
GGGTCAAGCCGATCCAGTCGCATGGGTGAGCTGCAAGACATTCAGGGTAAAGACGACAAGTGGAGCGTCCGCT
GACTGTTTCGTGGCAAGAGCGCTGATATCCATTACCAAGTCAGCGTCGACTGCAAGGCCGGTATGGCCGAGTACCA
ACGCCGTACATGAGCAATCCGTACCAGCGTGGTCC

YebF

LCC

GAATCCGACCCGACGCGCTGACCGCGGACGGCCGTTACGCGTGGCAACCTATACCGTGAGCCGCTTGAGCGT
GAGCGGTTTTGGTGGCGGCTTATCTATTACCCGACGGGCACGAGCCTGACCTTCGGTGGCATTGCAATGTCTCCG
GGTTACACGGCAGATGCGAGCTCTTAGCGTGGCTGGGTCGCCGCTGGCCTCGCACGGCTTTGTAGTTTTGGTGA
TCAACACTAATAGCCGTTTTGACTATCCGGACTACGTGCGTCCCAGCTGAGCGCGGCACTGAATATCTGCGTAC
GTCCAGCCCGAGCCGTTTCGTGCGCGCTTGGATGCGAATCGTCTGGCCGTCGCGGGTCACAGATGGGTGGCGG
CGGCACGCTGAGAATCGCGGAGCAAAACCCGTCCTTAAAGCTGCGGTGCCGCTGACCCCTTGGCACACCGATAA
AACCTTCAATACCTCTGTGCCGTTCTGATTGTGCGGTGCTGAAGCGGATACGGTTCGACCCAGTCAAGCAGCATGCA
ATTCCGTTTTATCAAATCTGCCGTCCACGACCCGAAAGTGTACGTTGAGCTGGATAATGCGAGCCACTTTGCAC
CGAATTCATAAACGCAGCCATCAGCGTGTACACCATCTCTTGATGAAGCTGTGGGTTGATAACGCACCCCGCTA
TCGTCAATTCTGTGTAACGTTAACGATCCGGCGCTGAGCGACTTTCGTACGAACAACCGTCACTGCCAGCATCAC
CATCATCACCCTGATAAGGTTGAGGTCTACCCCAAGGGCGACACCCCTAATTAGCCCGG

6xhistidine tag

CGAAAGGCCAGTCTTTCGACTGAGCCTTTCGTTTTATTTGATGCTGGCAGTTCCTACTCTCGCATGGGGAGTCC
CCACACTACCATCGGCGCTACGGCGTTTCACTTCTGAGTTCGGCATGGGGTCAGGTGGGACCACCGCGCTACTGCC
GCCAGGCAACAAGGGGTGTTATGAGCCATATTCAGGTATAAATGGGCTCGCGATAATGTTTCAAGATTGGTTAATT
GGTTGTAACACTGACCCCTATTTGTTATTTTTCTAAATACATTCAAATATGTATCCGCTCATGAGACAATAACCC
GATAAATGCTTCAATAATATTGAAAAAGGAAGAATATGAGCCATATTC AACGGGAAACGTCGAGGCCGCGATTAA
ATTCACATGGATGCTGATTTATATGGGTATAAATGGGCTCGCGATAATGTCGGGCAATCAGGTGCGACAATCTA
TCGCTTGTATGGGAAGCCGATGCGCCAGAGTTGTTTCTGAAACATGGCAAAAGGTAGCGTTGCCAATGATGTTACA
GATGAGATGGTCACTAAACTGGCTGACGGAATTTATGCCACTTCCGACCATCAAGCATTTTATCCGTAATCCTG
ATGATGCATGGTACTCACCCTGCGATCCCCGAAAAACAGCGTTCCAGGTATTAGAAGAATATCCTGATTCAGG
TGAAAAATATTGTTGATGCGCTGGCAGTGTCTGCGCCGTTGCACTCGATTCTGTTGTAATTGTCCTTTTAAACA
GCGATCGCGTATTTCCGCTCGCTCAGGCGCAATCACGAATGAATAACGGTTTGGTTGATGCGAGTGATTTGATGA
CGAGCGTAATGGCTGGCCTGTTGAACAAGTCTGGAAAGAAAATGCATAAACTTTTGCCATTCTCACCGGATTCACTC
GTCACTCATGGTGAATTTCTCACTTGATAACCTATTTTTGACGAGGGGAAATTAATAGGTTGATTTGATGTTGGACG
AGTCGGAATCGCAGACCGATACCAGGATCTTGCCATCCTATGGAAGTGCCTCGGTGAGTTTTCTCCTTATTACAG

Supporting Information

AAACGGCTTTTTCAAAAATATGGTATTGATAATCCTGATATGAATAAATTGCAGTTTCATTTGATGCTCGATGAGTT
TTTCTAAGCGGCGGCCATCGAATGGCGCAAAACCTTTCGCG

Kanamycin resistance

GTATGGCATGATAGCGCCCGGAAGAGAGTCAATTCAGGGTGGTGAATATGAAACCAGTAACGTTATAACGATGTCG
CAGAGTATGCCGGTGTCTCTTATCAGACCGTTTCCCGCGTGGTGAACCAGGCCAGCCACGTTTCTGCGAAAACGCG
GGAAAAAGTGAAGCGGCGATGGCGGAGCTGAATTACATTCCAACCGCGTGGCACAACAACCTGGCGGGCAAAC
AGTCGTTGCTGATTGGCGTTGCCACCTCCAGTCTGGCCCTGCACGCGCCGTCGCAAATTGTCGCGGCGATTAAATC
TCGCGCCGATCAACTGGGTGCCAGCGTGGTGGTGTGATGGTAGAACGAAGCGGCGTCGAAGCCTGTAAAGCGGC
GGTGCACAATCTTCTCGCGCAACGCGTCAGTGGGCTGATCATTAACTATCCGCTGGATGACCAGGATGCCATTGCT
GTGGAAGCTGCCTGCACTAATGTTCCGGCGTTATTCTTGATGTCTCTGACCAGACACCCATCAACAGTATTATTT
CTCCCATGAGGACGGTACGCGACTGGGCGTGGAGCATCTGGTCGCATTGGGTCACCAGCAAATCGCGCTGTTAGC
GGGCCCATTAAGTTCTGTCTCGGCGCGTCTGCGTCTGGCTGGCTGGCATAAATATCTCACTCGCAATCAAATTCAG
CCGATAGCGGAACGGGAAGGCGACTGGAGTGCCATGTCCGGTTTTCAACAAACCATGCAAATGCTGAATGAGGGC
ATCGTTCCCACTGCATGTCTGGTTGCCAACGATCAGATGGCGCTGGGCGCAATGCGCGCCATTACCGAGTCCGGGC
TGCGCGTTGGTGC GGATATCTCGGTAGTGGGATACGACGATACCGAAGATAGCTCATGTTATATCCCGCCGTTAAC
CACCATCAAACAGGATTTTCGCTGCTGGGGCAAACAGCGTGGACCGCTTGCTGCAACTCTCTCAGGGCCAGGGC
GTGAAGGGCAATCAGCTGTTGCCAGTCTCACTGGTAAAAGAAAACCACCCTGGCGCCCAATACGCAAACCGCC
TCTCCCCGCGCGTTGGCCGATTCAATATGCAGCTGGCACGACAGGTTTCCCGACTGGAAAGCGGGCAGTGA

Lac repressor

Figure S18. Plasmid sequence for pD421-*YebF*-WT-LCC. Kanamycin resistance (red), lac repressor (purple), *origin* (yellow), T5 promoter (grey), *6xHistidine tag* (magenta), *YebF* (cyan) and LCC (green). The plasmid map is shown in Figure S17.

Supporting Information

Figure S19. Structural alignment of LCC crystal and AlphaFold3-predicted models

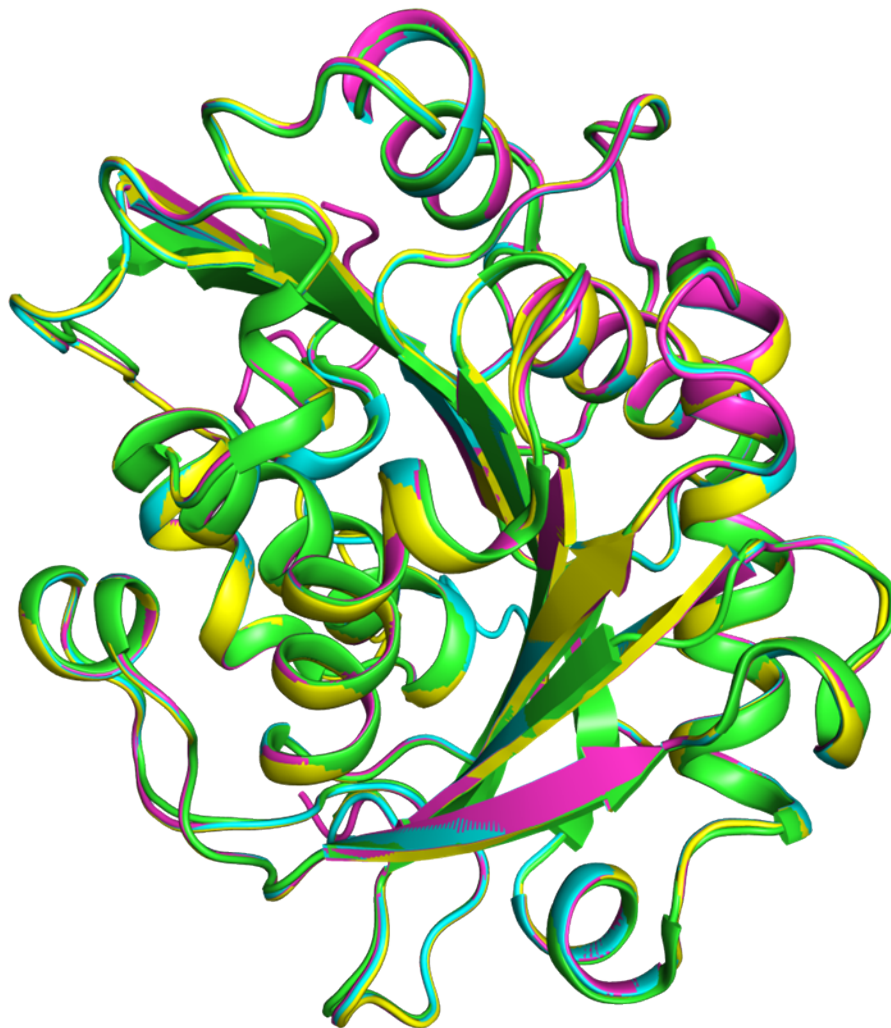


Figure S19. Structural alignment of LCC crystal and AlphaFold3-predicted models. The crystal structure of wild-type (WT) LCC (PDB ID: 4EB0, green) was superimposed with AlphaFold3-predicted structures of WT (cyan), V212T (magenta), and L102F/V212T (yellow) variants. The root-mean-square deviation (RMSD) values relative to the crystal structure were 0.3369 Å, 0.318 Å, and 0.3352 Å, respectively.